

A surface potential-based non-charge-sheet core model for undoped surrounding-gate MOSFETs*

He Jin(何进)^{1,2,3,†}, Zhang Jian(张健)², Zhang Lining(张立宁)², Ma Chenyue(马晨月)²,
and Chan Mansun(陈文新)³

(1 The Key Laboratory of Integrated Microsystems, Peking University Shenzhen Graduate School,
Shenzhen 518055, China)

(2 TSRC and ULTRAS Team, EECS, Peking University, Beijing 100871, China)

(3 Department of Electronics and Computer Engineering, Hong Kong University of Science & Technology,
Hong Kong, China)

Abstract: A surface potential based non-charge-sheet core model for cylindrical undoped surrounding-gate (SRG) MOSFETs is presented. It is based on the exact surface potential solution of Poisson's equation and Pao-Sah's dual integral without the charge-sheet approximation, allowing the SRG-MOSFET characteristics to be adequately described by a single set of the analytic drain current equation in terms of the surface potential evaluated at the source and drain ends. It is valid for all operation regions and traces the transition from the linear to saturation and from the sub-threshold to strong inversion region without fitting-parameters, and verified by the 3-D numerical simulation.

Key words: non-classical MOS transistor; surrounding-gate MOSFETs; device physics; surface potential model; non-charge-sheet approximation

DOI: 10.1088/1674-4926/30/2/024001

PACC: 7340Q

EEACC: 2560B; 2570D

1. Introduction

Extensive studies on surrounding-gate (SRG) metal-oxide-semiconductor field effect transistor (MOSFET) modelling have been performed in recent years and the related device physics have been well described by many different models^[1-6]. In the channel potential-based SRG-MOSFET models, the closed form current models are presented in terms of the intermediate variables or the potentials of the surface and centre point at the source and drain ends^[3-5]. In the charge-based SRG-MOSFET model^[6], semi-empirical charge expression is developed for SRG-MOSFETs based on a smooth function and interpolation. In Ref.[7], a unified charge-based model, valid for both heavily doped and intrinsic channel, is proposed. In addition, a carrier-based approach is found to be useful in developing generic compact model for SRG-MOSFETs^[8]. However, considerable attention has been focused on developing surface potential-based models in recent compact model formulations^[9,10]. At present, there is a general consensus that the surface potential approach not only includes as much device physics as possible but also retains high accuracy and model continuity.

In this paper, we propose an analytical surface potential-based non-charge-sheet core model for obtaining the $I_{ds}(V_{gs}, V_{ds})$ characteristics of the SRG-MOSFET, based on closed-form solutions of Poisson's equation, and Pao-Sah's dual integral equation. We demonstrate that an analogous formula

proposed by Brews *et al.* for the single-gate (SG) Bulk MOSFET^[11], can be carried out for the SRG-MOSFETs. The model has three distinctive features: (i) A single set of the surface potential voltage equation is obtained from the exact Poisson equation solution in the undoped SRG-MOSFET structure, analogous to that of the bulk MOSFETs, for which the complete surface potential equation is the beginning to develop a continuous model; (ii) The drain current, obtained from Pao-Sah's dual integral, is described by one continuous function in terms of the surface potentials at the source and drain, tracing properly the transition between different SRG-MOSFET operation regions without resorting to non-physical fitting-parameters; (iii) The charge-sheet approximation, typically used in bulk MOSFET models to simplify the Pao-Sah's equation for the current^[11,12], is not invoked, properly capturing SRG-MOSFET's volume inversion effect^[6]. The presented core model is ideally suited for being a base of SRG-MOSFET compact model development. In order to complete the model, short-channel effects, quantum effects, low and high field transport, and more, will be added in near future.

2. Model derivation

Let us consider an ideal long channel undoped n-type SRG-MOSFET, also note that only the electron term is considered. This simplification applies when $q\phi/kT \gg 1$, being the hole density negligible. Figure 1 shows the SRG-MOSFET structure, coordinate and energy band diagrams. Following

* Project supported by the National Natural Science Foundation of China (No. 60876027), a Competitive Earmarked Grant from the Research Grant Council of Hong Kong SAR (No. HKUST6289/04E), and the International Joint Research Program from Japan (No. NED005/06.EG01).

† Corresponding author. Email: frankhe@pku.edu.cn

Received 20 May 2008, revised manuscript received 26 October 2008

© 2009 Chinese Institute of Electronics

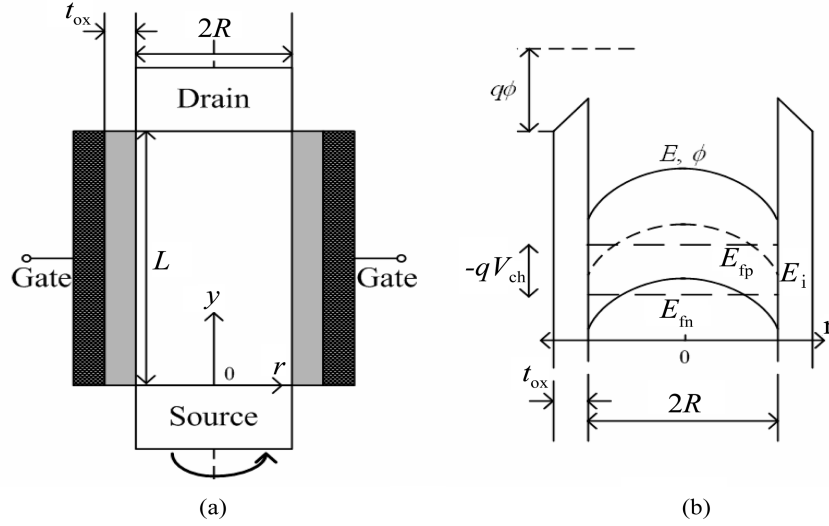


Fig.1. (a) Schematic cross section of an SRG MOSFET showing the coordinate system and relate variables; (b) Energy band diagram of an SRG MOSFET under certain V_{gs} and V_{ds} . E_{fp} is the hole quasi-Fermi level; E_{fn} is the electron quasi-Fermi level, and E_i is the intrinsic Fermi level.

the gradual-channel-approximation (GCA), Poisson's equation takes the one-dimensional (1-D) form^[3-5]:

$$\frac{d^2\phi}{dr^2} + \frac{1}{r} \frac{d\phi}{dr} = \frac{kT}{qL_D^2} \exp \frac{q(\phi - V)}{kT}, \quad (1)$$

where all symbols have common physics meanings. V is the quasi-Fermi-potential with $V = 0$ at the source end and $V = V_{ds}$ at the drain end. $L_D^{-2} = q^2 n_i / kT \epsilon_{si}$ is the reciprocal of the square of the intrinsic silicon Debye length. $\frac{kT}{q}$ is the thermal voltage and r is the spatial coordinate

Equation (1) must satisfy the following boundary conditions:

$$\left. \frac{d\phi}{dr} \right|_{r=0} = 0, \quad \phi(r=0) = \phi_0, \quad \phi(r=R) = \phi_s. \quad (2)$$

Equation (1) can be analytically solved yielding^[4,5]:

$$\phi_s = \phi_0 - \frac{2kT}{q} \ln \left[1 - \frac{R^2}{8L_D^2} \exp \frac{q(\phi_0 - V)}{kT} \right], \quad (3)$$

and

$$\left. \frac{d\phi}{dr} \right|_{r=R} = \frac{RkT}{2qL_D^2} \frac{\exp \frac{q(\phi_0 - V)}{kT}}{\left[1 - \frac{R^2}{8L_D^2} \exp \frac{q(\phi_0 - V)}{kT} \right]}. \quad (4)$$

From Gauss's law, the following relation must hold:

$$C_{ox}(V_{gs} - \Delta\varphi - \phi_s) = Q = \epsilon_{si} \left. \frac{d\phi}{dr} \right|_{r=R}, \quad (5)$$

where $C_{ox} = \epsilon_{ox} / [R \ln(1 + t_{ox}/R)]$ and $\Delta\varphi$ is the work-function difference. In the following discussion the mid-gap gate material, i.e., $\Delta\varphi = 0$, is assumed.

Substituting Eqs.(3) and (4) into Eq.(5) leads to

$$C_{ox}(V_{gs} - \Delta\varphi - \phi_s) = \frac{\sqrt{2}\epsilon_{si}kT}{qL_i} \exp \left[\frac{q(\phi_s - V)}{2kT} \right] \sqrt{1 - \exp \left[-\frac{q(\phi_s - \phi_0)}{2kT} \right]}. \quad (6)$$

Again, substituting Eq.(3) into Eq.(6) leads to

$$C_{ox}(V_{gs} - \Delta\varphi - \phi_s) = \frac{R\epsilon_{si}kT^2}{2qL_i^2} \exp \frac{q(\phi_s + \phi_0 - 2V)}{2kT}. \quad (7)$$

From Eq.(7), we obtain the centric potential expression:

$$\phi_0 = 2V - \phi_s + \frac{2kT}{q} \ln \frac{2L_i^2 C_{ox} q (V_{gs} - \Delta\varphi - \phi_s)}{R\epsilon_{si}kT}. \quad (8)$$

Equation (8) is submitted to Eq.(3), we have

$$\frac{q(V_{gs} - \Delta\varphi - \phi_s)}{kT} \left[\frac{1}{R} + \frac{qC_{ox}(V_{gs} - \Delta\varphi - \phi_s)}{4\epsilon_{si}kT} \right] = \frac{\epsilon_{si}}{2L_i^2 C_{ox}} \exp \frac{q(\phi_s - V)}{kT}. \quad (9)$$

Equation (9) is a fully rigorous surface potential-voltage equation of the SRG MOSFETs, which can be solved by a Newton-Raphson (NR) method to get the accurate surface potential value. In order to test the analytic surface potential model, we have compared the Eq.(9) prediction result of long-channel SRG-MOSFETs with the numerical simulations from DESSIS-ISE[®]. We have assumed a channel length (L) of 1 μm , silicon oxide thickness (t_{ox}) of 2 nm, and a mid-gap gate structure. A constant effective mobility of 400 $\text{cm}^2/(\text{V}\cdot\text{s})$ has been used for both calculations.

To apply Eq.(9) to current and charge modelling, ϕ_s needs to be evaluated at the source ($y = 0$) and drain ($y = L$) ends with $V = 0$ and $V = V_{ds}$, respectively. The results are separately labelled as $\phi_s = \phi_{SS}$ and $\phi_s = \phi_{SL}$. Figure 2 shows the surface potential versus gate voltage curves calculated from Eq.(9) for the source and drain ends, compared with the 3-D simulation. The solution, given by Eq.(9), is continuously and smoothly valid for all regions of the SRG-MOSFET operation. It is found that the results from Eq.(9) agree with the 3-D in all operation regions for both the source and drain potentials.

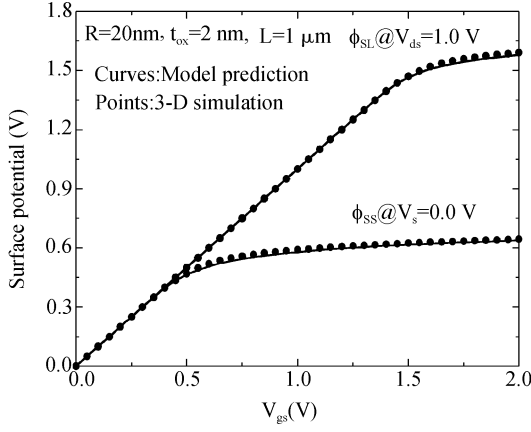


Fig.2. Comparison of source and drain end surface potential obtained from Eq. (9) (solid lines) with the 3-D numerical result (points).

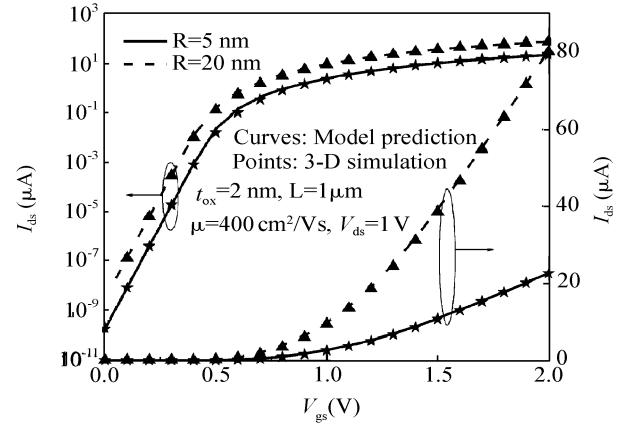


Fig.4. Transfer characteristics obtained from the surface potential-based model for two silicon film radius (solid and dashed lines), compared with numerical simulations from DESSIS-ISE[®] (points).

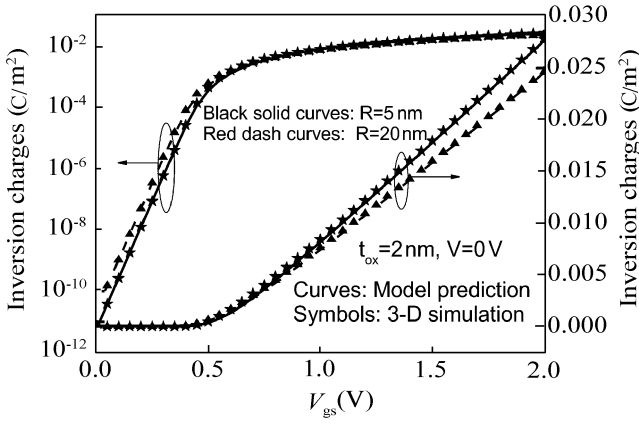


Fig.3. Inversion charge characteristics obtained from Eq. (5) (solid and dash lines) based on calculated surface potential, compared with the 3-D numerical simulation (points).

Figure 3 compares the inversion charge density between the model prediction and the 3-D simulation for different silicon body radii. It is observed from Fig.3 that the model and simulation agree well. In addition, the sub-threshold charge increases as the silicon radius increases, and a unique “volume inversion effect” is also predicted from the presented model, coinciding with non-classical MOSFET device physics.

For a given V_{gs} , ϕ_s can be solved from Eq.(9) as a function of V . Note that V varies from the source to the drain. The functional dependence of $V(y)$ and $\phi_s(y)$ is determined by the current continuity equation, which requires the SRG-MOSFET drain current $I_{ds} = \mu(2\pi R)QdV/dy = \text{constant}$, independent of V or y . The parameter μ is the effective mobility. Following Pao–Sah’s dual integral^[11], integrating

$$I_{ds} = \frac{2\pi R\mu C_{ox}}{L} \int_{\phi_s}^{\phi_d} \left[(V_{gs} - \Delta\varphi - \phi_s) + \frac{kT}{q} - \frac{kT}{qR} \left(\frac{1}{R} + \frac{C_{ox}q(V_{gs} - \Delta\varphi - \phi_s)}{4\epsilon_{si}kT} \right)^{-1} \right] d\phi_s. \quad (11)$$

The integration of Eq.(11) is performed analytically to yield:

$$I_{ds} = \frac{2\pi R\mu C_{ox}}{L} \left\{ (V_{gs} - \Delta\varphi)\phi_s - \frac{\phi_s^2}{2} + \frac{kT\phi_s}{q} + \left(\frac{kT}{q} \right)^2 \frac{4\epsilon_{si}}{RC_{ox}} \ln \left[\frac{1}{R} + \frac{C_{ox}q(V_{gs} - \Delta\varphi - \phi_s)}{4\epsilon_{si}kT} \right] \right\} \Bigg|_{\phi_{SS}}^{\phi_{SL}}. \quad (12)$$

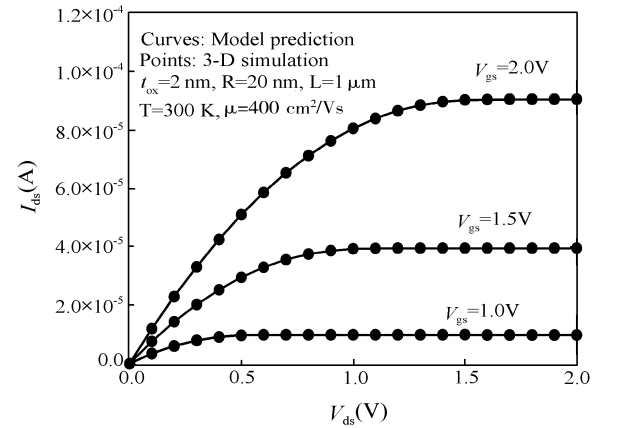


Fig.5. Output characteristics obtained from the surface potential model (solid lines) compared with numerical simulations from DESSIS-ISE[®] (points).

$I_{ds}dy$ from the source to the drain and expressing dV/dy as $(dV/d\phi_s)(d\phi_s/dy)$, the non-charge-sheet drain current is written as

$$I_{ds} = \mu \frac{2\pi R}{L} \int_0^{V_{ds}} Q(V)dV = \mu \frac{2\pi R}{L} \int_{\phi_{SS}}^{\phi_{SL}} Q(\phi_s) \frac{dV}{d\phi_s} d\phi_s, \quad (10)$$

where ϕ_{SS}, ϕ_{SL} are solutions to Eq.(9) corresponding to $V = 0$ and $V = V_{ds}$, respectively. By using Eq.(9) and replacing it into $Q = C_{ox}(V_{gs} - \phi_s)$, the total mobile charge per unit gate area expressed in terms of ϕ_s yields $Q(\phi_s)$. Note that $dV/d\phi_s$ can also be expressed as a function of ϕ_s by differentiating Eq.(9). Substituting these factors in Eq.(10), we have

3. Result and discussion

From Eq.(12), the SRG-MOSFET drain current can be easily computed. In the following, the SRG-MOSFET operation regions are derived from this continuous surface potential based analytical model:

(i) Linear region above threshold. In this region the drift current component dominates the device performance. Hence, we observe that the total drain current can be approximated by first two terms only above the threshold as shown in Eq.(13).

$$I_{ds} \approx \frac{2\pi R\mu C_{ox}}{L} \left[(V_{gs} - \Delta\varphi)(\phi_{SL} - \phi_{SS}) - \frac{1}{2}(\phi_{SL}^2 - \phi_{SS}^2) \right]. \quad (13)$$

This current expression is just drift component of the traditional surface-potential-based bulk MOSFET models, thus dominates in the strong inversion region;

(ii) Sub-threshold region: Below threshold the SRG MOSFET current picture has a little difference from the bulk MOSFET model. Here, the first two components are negligible and the negative fourth component cancels a half of third component in this region. As a result, the total drain current is described by

$$I_{ds} \approx \frac{2\pi R\mu C_{ox}}{L} \left[\frac{2kT}{q}(\phi_{SL} - \phi_{SS}) + \left(\frac{kT}{q} \right)^2 \frac{4\epsilon_{si}}{RC_{ox}} \ln \frac{4\epsilon_{si}kT + C_{ox}qR(V_{gs} - \Delta\varphi - \phi_{SL})}{4\epsilon_{si}kT + C_{ox}qR(V_{gs} - \Delta\varphi - \phi_{SS})} \right]. \quad (14)$$

This drain expression can be simplified into

$$I_{DS} = \mu \frac{\pi R^2}{L} n_i kT \exp \frac{q(V_{gs} - \Delta\varphi)}{kT} \left(1 - \exp \frac{-qV_{ds}}{kT} \right). \quad (15)$$

The sub-threshold current in Eq.(15) is proportional to the cross-sectional area of the SRG-MOSFET and independent of t_{ox} . This is a characteristic of the volume inversion effect that cannot be captured by standard charge-sheet based models;

(iii) Saturation region. This regime occurs when the contribution of the drain end to the drain current is a little. Hence, the drain current is expressed as

$$I_{ds} = \mu \frac{\pi R}{L} \left(Q_s + \frac{C_{ox}kT}{q} \right) (\phi_{SL} - \phi_{SS}). \quad (16)$$

The saturation current mainly depends on the source inversion charge density as expected for an MOSFET.

In order to verify the presented drain current model, the drain current curves between the model prediction and the 3-D simulation are also compared as done for the surface and inversion charge. Figure 4 shows the SRG-MOSFET transfer curves, and Figure 5 plots the SRG-MOSFET output curves,

calculated from the surface potential-based model and the 3-D numerical simulation. Again, good agreement is observed without using any fitting parameter in both figures. Especially, the volume inversion effect of SRG-MOSFET demonstrated in Fig.4 is well described by the presented model, matching the 3-D numerical simulation.

4. Conclusion

In summary, we have presented an analytical surface potential-based current-voltage model suitable for compact modeling of undoped (lightly doped) SRG-MOSFETs. All the operation regions and the transitions are correctly described by preserving the physics. In particular, the volume inversion effect, that cannot be captured by using the traditional charge-sheet approximation, is well accounted of in this model.

References

- [1] Colinge J P. Multiple-gate SOI MOSFETs. *Solid-State Electron*, 2004, 48(6): 897
- [2] Iniguez B, Fjeldly T A, Lazaro A, et al. Compact-modeling solutions for nanoscale double-gate and gate-all-around MOSFETs. *IEEE Trans Electron Devices*, 2006, TED-53(9): 2128
- [3] Jiménez D, Iniguez B, Suñé J, et al. Continuous analytic current-voltage model for surrounding gate MOSFETs. *IEEE Electron Device Lett*, 2004, 25(8): 571
- [4] Wei B, He J, Tao Y, et al. An analytic potential-based model for undoped nanoscale surrounding-gate MOSFETs. *IEEE Trans Electron Devices*, 2007, 54(9): 2293
- [5] He J, Zhang J, Zhang L, et al. A complete analytical surface potential-based core model for undoped cylindrical surrounding-gate MOSFETs. *Proc NSTI-Nanotech*, 2008: 598
- [6] Iniguez B, Jimenez D, Roig J, et al. Explicit continuous model for long-channel undoped surrounding-gate MOSFETs. *IEEE Trans Electron Devices*, 2005, 52(8): 1868
- [7] Liu F, He J, Zhang L, et al. A charge-based model for long-channel cylindrical surrounding-gate MOSFETs from intrinsic channel to heavily doped body. *IEEE Trans Electron Devices*, 2008, 55(8): 2187
- [8] He J, Chan M, Zhang X, et al. A carrier-based analytic model for the undoped (lightly doped) cylindrical surrounding-gate MOSFETs. *Solid-State Electron*, 2006, 50(4): 416
- [9] SRC. Request for white papers: semiconductor device compact modeling for circuit design. April 23, 2003. <http://www.src.org>
- [10] CMC website of Next Generation MOSFET Model Standard Phase-III Evaluation Results. <http://www.eigroup.org/CMC>
- [11] Brews J R. A charge sheet model of the MOSFET. *Solid-State Electron*, 1978, 21: 345
- [12] Pao H C, Sah C T. Effects of diffusion current on characteristics of metal-oxide (insulator)-semiconductor transistors. *Solid-State Electron*, 1966, 9: 927